AIAA

AEROSPACE SCIENCES MEETING
NEW YORK, NEW YORK
JANUARY 20-22, 1964

CURRENT DISTRIBUTIONS IN LARGE-RADIUS PINCH DISCHARGES

by

R. G. JAHN and W. von JASKOWSKY
Princeton University
Princeton, New Jersey

Preprint No.
64-25

CURRENT DISTRIBUTIONS IN LARGE-RADIUS PINCH DISCHARGES

Robert G. Jahn
Assistant Professor of Aeronautical Engineering
and
Woldemar von Jaskowsky
Research Staff Member
Guggenheim Laboratories for the Aerospace Propulsion Sciences
Princeton University, Princeton, New Jersey

Abstract

In an effort to understand more fully the basic mechanisms of gas acceleration in pulsed plasma devices, a series of detailed magnetic probe experiments has been performed on a variety of large-radius linear pinch discharges.[1] From the space and time variations of the interior magnetic fields thus determined, the concomitant distributions of current density within the discharges have been evaluated. For example, in argon at initial pressures between 20μ and 3 mm., a 10 KV, 230 KC pulse from a 15 μfd capacitor bank is found to generate well-defined cylindrical sheets of current which propagate radially inward from the periphery of the electrodes. The observed radius-time trajectories of these sheets, and those of the accompanying luminous fronts have been compared with theoretical snow-plow calculations, and are found to be reconcilable if some fractional "sweeping efficiency" is assigned to each of the observed current sheets. The applicability of the scaling laws implicit in the snow-plow formulation has been explored experimentally by changing the initial pressure, the type of gas, the radius of the discharge, the capacitance and voltage of the external bank, and the inductance of the external circuit.

Introduction

The research described in this paper is part of a detailed experimental and theoretical study of various physical processes occurring in a large-radius pinch discharge. Of particular interest are those details of the breakdown initiation, current sheet stability, and magnetogasdynamic acceleration which seem generally relevant to various pulsed plasma propulsion devices. The apparatus employed in the experiments has been developed to generate reproducible, stable, geometrically simple discharges in a form accessible to detailed study. This apparatus, and some earlier experimental results have been described in detail in a previous article.[1] Briefly, the central device is an aluminum discharge chamber, with plane circular electrodes of 4 or 8-in. diameter, separated by a 2-in. gap of test gas at some prescribed pressure (Figs. 1, 2). The discharge is driven by a circular bank of 15 1.0 μfd capacitors charged to 10,000 v., ringing down through a low inductance circuit via a gas-triggered inverse pinch switch, also described in detail elsewhere.[2] Terminal measurements with a voltage divider and Rogowski coil indicate that the discharge current rises at about 5×10^{11} amp/sec to a peak value of 200,000 amperes from which it rings down at about 230 KC, developing some 10% of the bank voltage across the electrode gap.

The luminous phenomena occurring during the discharge are observed by rotating mirror streak photographs taken along a diameter of the chamber, and by single-frame Kerr cell photographs taken through special glass electrodes[1], at selected times. Fig. 3 shows a typical streak photograph of an 8-in. diameter discharge in 20μ argon. The breakdown is seen to initiate at the outer edge of the electrodes, presumably as a peripheral ring, and then to accelerate inward. Subsequent discharges occurring near the times of current reversal in the ringdown pattern are also established at the outer edge of the electrodes, and follow the first luminous front in toward the center.

Full-field Kerr cell photographs, such as those shown in Fig. 4, verify that the luminous fronts are cylindrical in structure, with little azimuthal aberration or tendency toward instability. The velocities of these luminous fronts are strong functions of the ambient gas pressure and molecular weight, and of the circuit parameters and chamber size. The correlation of their trajectories with the experimentally determined current density and magnetic field distributions, and with a theoretical model is the main topic of this paper.

Current Density Distributions

The phenomenological observations of the progress of the luminous fronts permit little interpretation until the development of the current density distributions, and their associated magnetic fields within the chamber are established. For this purpose, magnetic probes of the conventional design[3] were introduced at various radial positions within the discharge, midway between the electrodes. These probes are constructed of 5 turns of 0.25 mm formvar wire, each about 5 mm^2 in cross section, enclosed in a 5 mm o.d. pyrex tube. The probe tubes are inserted

radially through the side wall insulator, past the chamber center line to the desired position on the far side of the chamber. That is, the luminous fronts pass over the probe envelopes from the nose side. Fig. 5 shows the response, $\frac{\partial B}{\partial t}(t)$ and the integrated response, B(t), of one such probe located at radii of 3.0 and 1.5 in. in a 4 in. radius discharge of 20μ argon. The series of sharp peaks on the $\frac{\partial B}{\partial t}$ records immediately indicates that the current density, like the luminosity, is localized in relatively thin sheets which propagate radially inward.

Detailed reduction of many magnetic probe records like that shown above, yield maps of the current density distribution as a function of radius at various times, in accordance with the appropriate statement of Maxwell's relation in cylindrical geometry:

$$\mu_0 j = \frac{1}{r}\frac{\partial}{\partial r}(Br)$$

A typical map of this sort, in this case for an 8-in. diameter discharge in 125μ argon is shown in Figs. 6a and 6b. The current density is seen to assemble itself into a fairly broad pulse near the outer edge, which then propagates inward at nearly constant amplitude for about 1½-in. At that time, about 2.2 μsec after breakdown, the current in the external circuit reverses, and a new pulse, of reverse polarity, arises at the outer wall. This second pulse, which also proceeds inward, is seen to be more sharply defined, and of greater amplitude than the first, even though the external circuit current is now less than during the first half cycle. The second pulse also propagates somewhat faster than the first and eventually reaches about half radius before being "short-circuited" by another re-reversal of external current. At this time, a corresponding third, positive discharge pulse forms back at the outer wall (not shown in Fig. 6b).

It is speculated that the second pulse owes its sharper definition and greater amplitude to the fact that it propagates into a body of gas already substantially ionized by the passage of the first current sheet, which itself enjoys no such advantage. The higher velocity of the second sheet may arise from a correspondingly higher $\vec{j} \times \vec{B}$ force acting on it, or from the fact that the first sheet has swept up some of the gas, leaving a lower density medium, which may also be convecting inward, ahead of the second sheet. Microwave probing of the region between the two sheets, currently in progress, hopefully will yield some information on the ionization level there.

Included in Fig. 6 are the trajectories of the luminous fronts for this type of discharge (solid lines), obtained from the streak photographs. The first luminous front is seen to propagate somewhat behind the first current pulse, at a somewhat lower velocity. The second luminous front, to the contrary, propagates a bit ahead of the second current sheet, at nearly the same velocity. The latter behavior is commensurate with the concept of a $\vec{j} \times \vec{B}$ "piston" pushing a body of hot gas; the former clearly is not.

Also included in Fig. 6 are the trajectories of the peaks of $\frac{\partial B}{\partial t}$ like those seen in Fig. 5. Wherever the radial current density variation is very steep, it seems reasonable to approximate $\frac{\partial B}{\partial r}$ by $\frac{1}{v}\frac{\partial B}{\partial t}$ where v is the convective speed of the pattern. If, in addition, this term substantially exceeds $\frac{B}{r}$, maxima in $\frac{\partial B}{\partial t}$ should then be indicative of maxima of current density, j. The utility of this approximation lies in providing a rapid indication of the current pulse trajectories, prior to the more tedious reduction of the complete probe records to full maps of the current density distribution. It is seen from Figs. 6a and 6b that this is a serviceable approximation in this case over most of the significant range of the two current sheets.

The final trajectory included in Figs. 6a and 6b, (dashed line) is that predicted theoretically for a "snow-plow" type piston. In this theory, it is assumed that the current sheet is infinitesimally thin, completely impermeable to the gas it pushes, and that the accelerated gas accumulates in an infinitesimally thin layer on the current sheet. This dynamical model is solved simultaneously with the circuit equation, and with the statement of coaxial cylindrical inductance, for trajectories, $r(t)$, of the current sheet, and for the ringdown pattern of the circuit. The details of this formulation are reviewed in the Appendix. Briefly, the problem is characterized by two dimensionless parameters, and a dimensionless time:

$$\alpha = -\frac{\mu_0 h}{2\pi L_0} \quad ; \quad \beta = -\frac{Q_0^2}{4\pi \rho_0 r_0^4} \quad , \quad T = t/\sqrt{L_0 C}$$

where

h = distance between electrodes
L_0 = initial circuit inductance
Q_0 = initial charge on capacitors
ρ_0 = initial gas density
r_0 = radius of discharge at inception
C = capacitance of bank
t = real time

The parameter α essentially reflects the ratio of discharge inductance to external circuit inductance. For the prevailing experimental values, the trajectory solutions are relatively insensitive to α, other than through the implicit time scaling in L_0. The parameter β, which reflects the ratio of accelerating $\vec{j} \times \vec{B}$ force to the mass of gas to be accelerated, is much more manifest in the form of the

solution. For large $|\beta|$ (>0.2) the current sheet reaches the center before the external current reverses. For small β, the external current reverses before the sheet reaches the center, a situation which we know experimentally causes a second breakdown at the periphery, thus clearly invalidating the theoretical model from that time.

Returning to Fig. 6, then, we note two interesting comparisons with the snow-plow trajectory for $\beta = -0.022$, the value prevailing in the experiment. First, over the first 2.2 μsec, where the theoretical model has some hope of applicability, the observed current pulse is substantially ahead of the snow-plow trajectory, and traveling faster than it. Rather, it is the luminous front which seems to correlate with the snow plow. Second, this apparently fortuitous correlation between the snow plow and luminous front persists long after the second breakdown, where the theory should be clearly inapplicable.

Scaling Properties

While a single set of experiments, such as that summarized in Fig. 6, leave the applicability of the snow plow concept considerably in doubt, the scaling relations such a formulation yields seem sufficiently general to warrant experimental exploration. To this end, a variety of discharges have been produced, covering a range of the β parameter from -.001 to -2.3. This variation can be achieved in several practical ways. Simplest is an adjustment of the initial gas density and molecular weight over the ranges where satisfactory discharges can be produced. To date, argon has been studied from 20μ to 10 mm, nitrogen from 20μ to 1 mm, and helium from 36μ to 10 mm. Other ambient gas conditions are currently under study.

The β parameter varies as the square of the charge on the capacitor bank, and thus as the square of the capacitance, or the applied voltage. A certain amount of this type of survey has been performed, and more is in progress. It should be noted, however, that variation in bank capacitance also alters the time scaling factor, and variation in bank voltage may conceivably alter the nature of the breakdown initiation. For these reasons, this mode of scaling may be less instructive than the others.

The most significant factor in the β parameter is the initial discharge radius, r_0, which appears in the inverse fourth power. By halving the radius of the discharge chamber, therefore, β is increased by a factor of sixteen, and substantial changes in the nature of the discharge should appear. To explore this, one of the 8-in. diameter chambers was converted to a 4-in. chamber by insertion of a suitable pyrex cylinder and plexiglas electrode shield. Discharges generated in this device were studied with the streak photography and magnetic probe techniques outlined above. The streak photographs reveal that the first luminous front is now much more intense, and propagates more rapidly, accelerating over its entire radial course, and reaching the center before current reversal in the external circuit. The secondary luminous fronts are relatively much less intense than in the larger chamber. The magnetic probe records indicate a similar intensification of the first current pulse in the 4-in. discharge, which is found to be narrower and steeper than the first pulse in the 8-in. machine, and to propagate all the way to the center. The secondary pulses produce much less pronounced responses on the magnetic probes.

The results in the 4-in. diameter discharges have stimulated design of a completely new device of this size which will have substantially lower external circuit inductance, and thereby a larger α parameter. Results from this machine may be available at the time of the talk.

Returning now to the correlation of the various experimental and theoretical trajectories, Fig. 7 attempts a summary of the luminous front data obtained from several of the many β—scaling experiments. Superimposed on each luminous front trajectory is a portion of the theoretical snow-plow calculation for the prevailing value of β, indicating that fortuitous as this correlation may be, it prevails over a broad range of experimental conditions.

Figs. 8a, 8b, 8c present superpositions of $\frac{\partial B}{\partial t}$ peak trajectories (indicative of current pulses as mentioned earlier), and snow-plow calculations. In most cases it is found that the current pulses propagate somewhat faster than the theoretical trajectory, a property which could be construed as a failure of the current pulse to accelerate all of the gas it overruns, i.e., to a "leakiness" of the piston. A "leaky snow-plow" theory would differ from the more conventional one only in the appearance of a "sweeping efficiency" factor, ξ, in the denominator of the β parameter, representing the fact that the piston only accumulates $\xi\rho_0$ of the original gas density as it propagates through it. Indeed, it is found that the snow-plow calculations can be brought into better coincidence with the experimental current pulse trajectories, if higher values of β are empirically invoked. For example, in an 8-in. discharge in 535μ argon (Fig. 8a), the experimental trajectory is found to correspond with the snow-plow trajectory for a value of β about 8 times that actually prevailing in the experiment, indicating only about 12% sweeping efficiency, ξ. For the same radius discharge at a lower pressure, 125μ (Fig. 8b), the correlation occurs for a theoretical β about twice that of the experiment, i.e., a 50% sweeping efficiency.

At the lowest ambient pressure employed, 20μ (Fig. 8c), the correlation is within experimental error without any adjustment of β, i.e., the current pulse piston here seems to be essentially impermeable.

Similar comparisons for the 4-in. diameter discharges in argon, where the current density pulses are much more intense, indicate essentially impermeable behavior at all pressures studied (20μ - 500μ argon). Correlation of the empirical sweeping efficiency with other relevant parameters of the discharge is in progress. It is suspected that the opacity of the current pulses may be conditioned as much by their mode of initiation as by their dynamical development, and thus dimensional criteria such as current rise time, initial voltage, ambient density and molecular details of the gas, not explicit in the snow-plow model, may be relevant.

Summary and Acknowledgements

The experiments described above have revealed the detailed structure of the cylindrical current pulses arising in a large radius pinch discharge, and the characteristics of their propagation toward the center. These have been compared with the trajectories of the associated luminous fronts, and with the predictions of a simple snow-plow theory. There appears to be a fortuitous correlation of the luminous front trajectories with the snow-plow formulation over a broad range of experimental conditions. The observed current pulse velocities tend in some cases to exceed the theoretical snow-plow values, suggesting a degree of "leakiness" in their piston action on the ambient gas. The sweeping efficiency seems to increase for lower ambient gas density, and for smaller discharge radius.

The authors gratefully acknowledge the work of Messrs. N. A. Black, R. Burton, J. Corr, and A. L. Casini in performing and interpreting many of the experiments. Mr. N. A. Black prepared the following Appendix.

Appendix: Snow-Plow Formulation of Pinch Dynamics[4]

Assume the discharge current to flow in one circular cylinder of infinitesimal thickness and infinite conductivity. Assume it collects all gas it passes over into one infinitesimally thin sheet coincident with itself. Let:

r = radius of current sheet, initial value r_o
L_o = inductance of external circuit
h = separation of electrodes
Q = charge on capacitors, initial value Q_o
ρ_o = ambient gas density

The complete circuit relation:

$$L\frac{d^2Q}{dt^2} + \frac{dL}{dt}\frac{dQ}{dt} + \frac{Q}{C} = 0 \qquad (1)$$

where the inductance,

$$L = L_o + \frac{\mu_o h}{2\pi}\ln\left(\frac{r_o}{r}\right) \qquad (2)$$

is to be solved simultaneously with the dynamical statement,

$$\frac{d}{dt}\left[(r_o^2 - r^2)\frac{dr}{dt}\right] = -\frac{\mu_o (dQ/dt)^2}{4\pi^2 \rho_o r} \qquad (3)$$

Defining the five dimensionless parameters,

$$\alpha = -\frac{\mu_o h}{2\pi L_o}$$

$$\beta = -\frac{Q_o^2}{4\pi^2 \rho_o r_o^4}$$

$$\tau = t/\sqrt{L_o C}$$

$$y = \frac{r}{r_o}$$

$$Z = \frac{Q}{Q_o}$$

yields the dimensionless circuit equation

$$\frac{d^2Z}{d\tau^2} + \frac{\alpha}{(1+\alpha \ln y)y}\frac{dy}{d\tau}\frac{dZ}{d\tau} + \frac{Z}{(1+\alpha \ln y)} = 0,$$

with initial conditions

$$Z = 1, \quad \frac{dZ}{d\tau} = 0 \quad \text{at } \tau = 0$$

JAWN-A

and the dimensionless momentum equation

$$\frac{d}{d\mathcal{T}}\left[(1-y^2)\frac{dy}{d\mathcal{T}}\right] = \frac{\beta}{y}\left(\frac{dz}{d\mathcal{T}}\right)^2 ,$$

with initial conditions

$$y = 1 \quad , \quad \frac{dy}{d\mathcal{T}} = 0 \quad \text{at} \quad \mathcal{T} = 0$$

These relations were evaluated on an IBM 7090 for $y(\mathcal{T})$, $z(\mathcal{T})$, $\frac{dy}{d\mathcal{T}}(\mathcal{T})$, $\frac{dz}{d\mathcal{T}}(\mathcal{T})$ for a physically interesting range of α and β.

References

1. R. G. Jahn and W. von Jaskowsky, "Structure of a Large-Radius Pinch Discharge", AIAA Jour., 1, No. 8, pp. 1809-1814, (1963).
2. R. G. Jahn, W. von Jaskowsky, and A. L. Casini, "Gas-Triggered Inverse Pinch Switch", Rev. Sci. Inst., 34, No. 12, (1963).
3. R. H. Lovberg, "The Use of Magnetic Probes in Plasma Diagnostics", Ann. of Phys. 8, 311-324, (1959).
4. M. Rosenbluth, "Infinite Conductivity Theory of the Pinch", Los Alamos Tech. Report LA-1850, (1954).

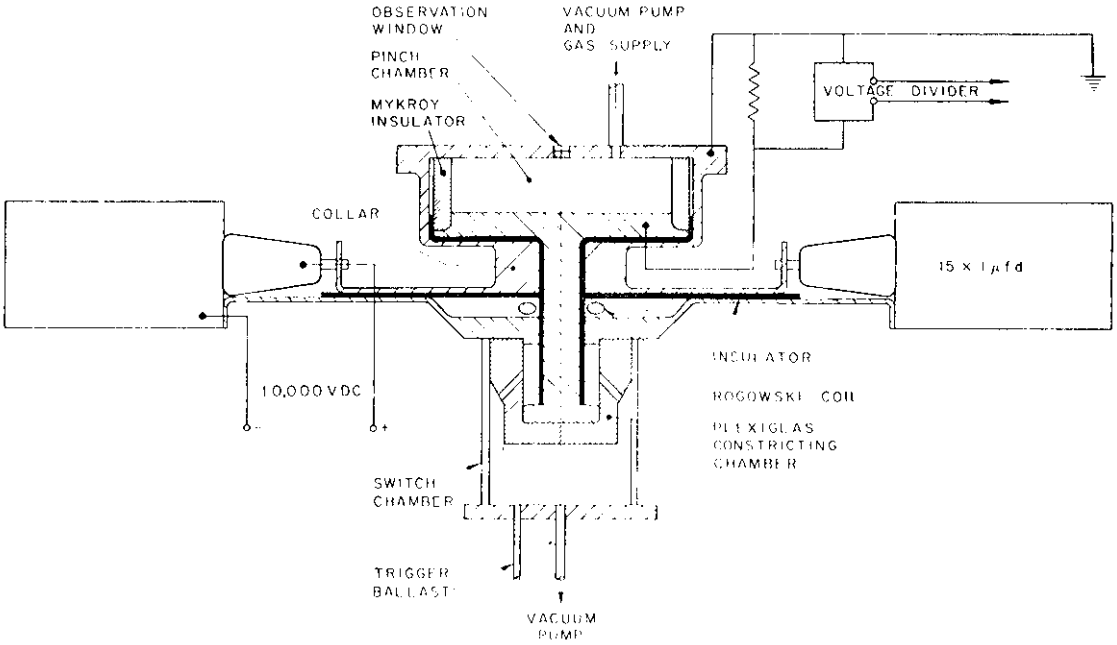

FIGURE 1 PLASMA PINCH APPARATUS (SCHEMATIC)

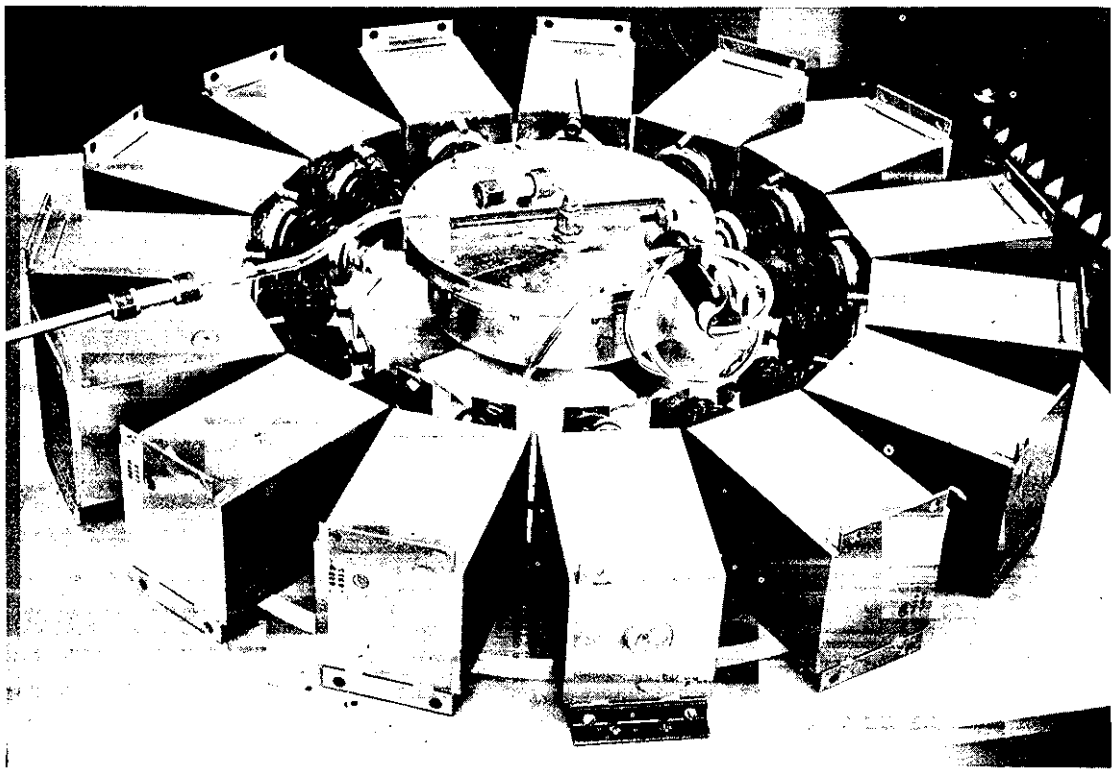

FIGURE 2

PLASMA PINCH APPARATUS

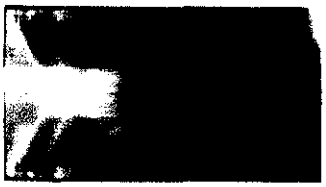

JAHN-6

FIGURE 3
STREAK PHOTOGRAPH OF PINCH DISCHARGE IN 20 μ ARGON

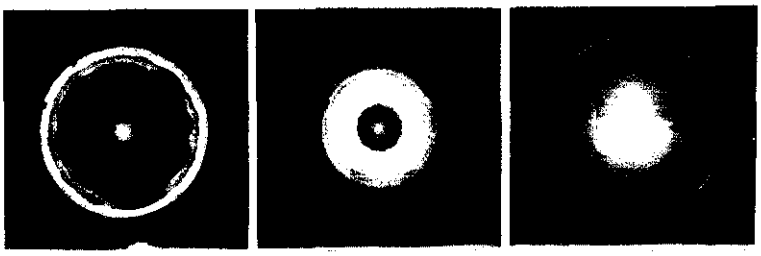

FIGURE 4
AXIAL PHOTOGRAPHS OF PINCH DISCHARGE
125 μ ARGON; 0.05 μ SEC EXPOSURE:
A: 2.3 μ SEC; B: 6.7 μ SEC; C: 11 μ SEC AFTER INCEPTION

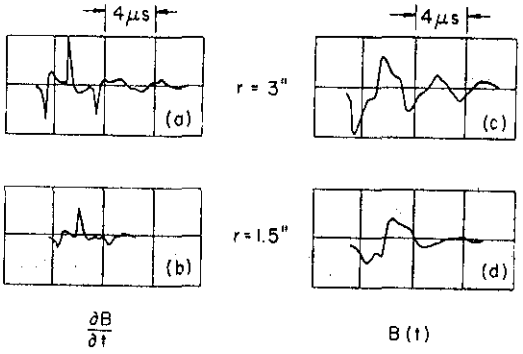

FIGURE 5
RESPONSE OF MAGNETIC PROBES TO PINCH DISCHARGE IN 20μ ARGON

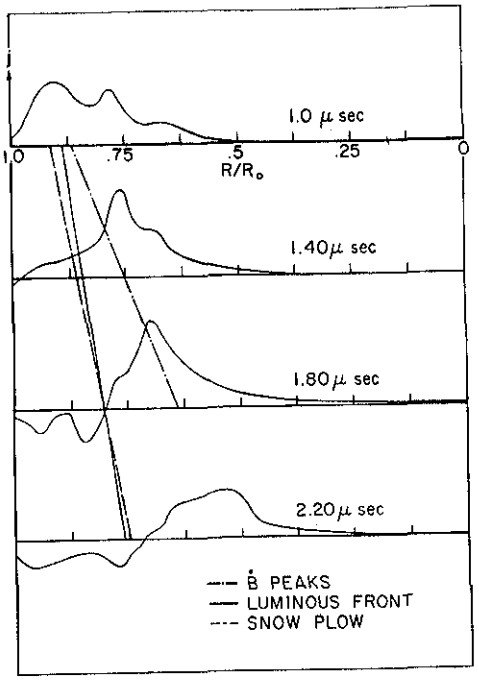

FIGURE 6a
RADIAL CURRENT DENSITY DISTRIBUTIONS IN 125μ ARGON PINCH DISCHARGE: 0-2.2μ sec

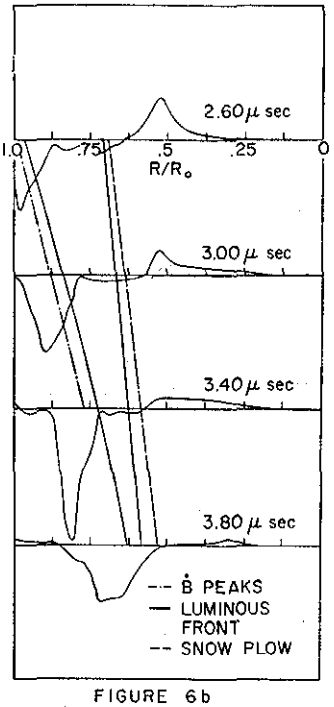

FIGURE 6b
RADIAL CURRENT DENSITY DISTRIBUTIONS IN 125μ ARGON PINCH DISCHARGE : 2.6-3.8μsec

JAHN 7

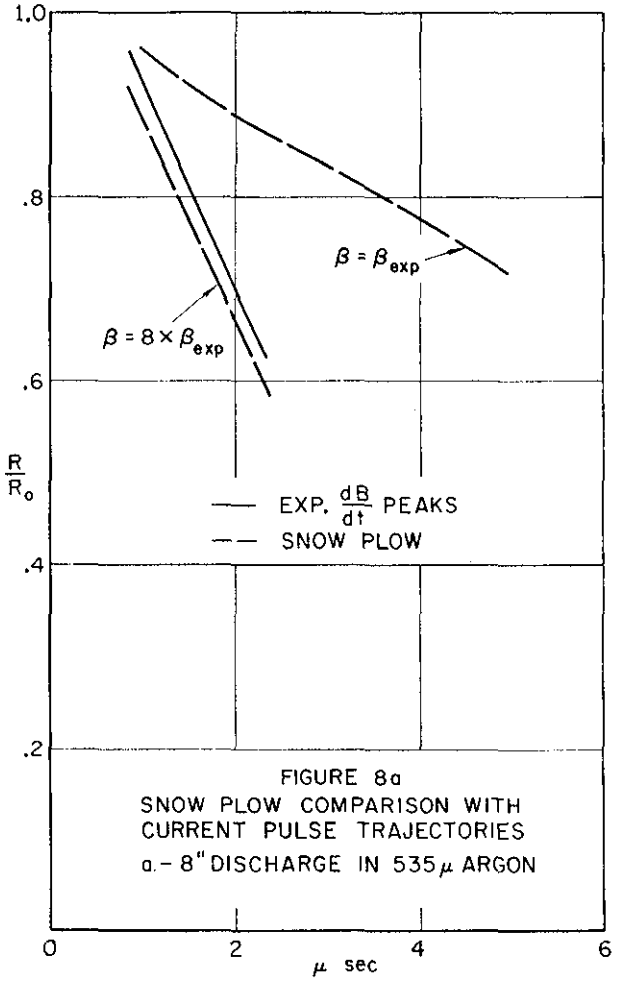

FIGURE 8a
SNOW PLOW COMPARISON WITH CURRENT PULSE TRAJECTORIES
a.- 8" DISCHARGE IN 535 μ ARGON

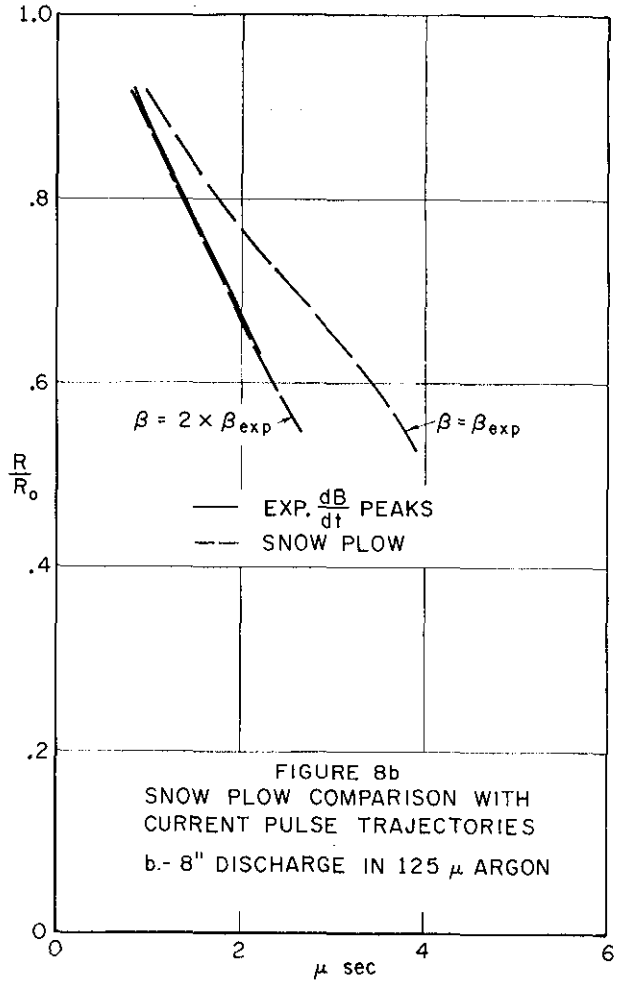

FIGURE 8b
SNOW PLOW COMPARISON WITH CURRENT PULSE TRAJECTORIES
b.- 8" DISCHARGE IN 125 μ ARGON

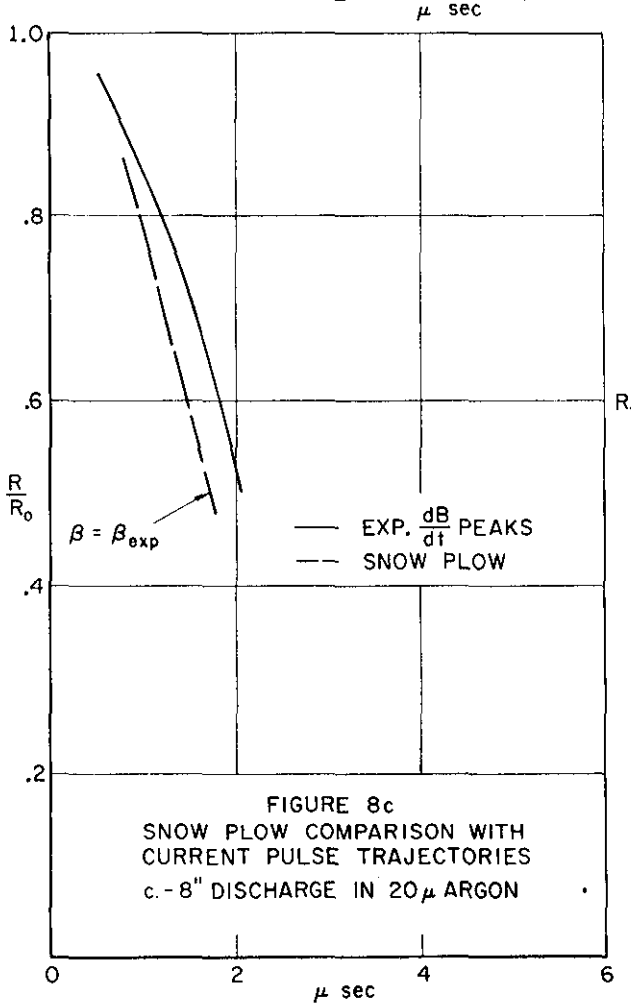

FIGURE 8c
SNOW PLOW COMPARISON WITH CURRENT PULSE TRAJECTORIES
c.- 8" DISCHARGE IN 20 μ ARGON

R 98

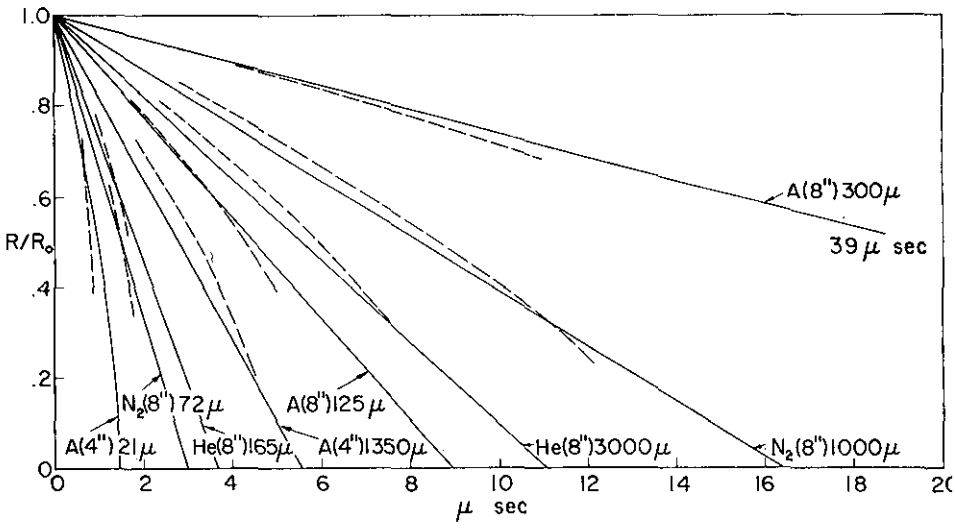

FIGURE 7
POSITION OF LUMINOUS FRONTS VS TIME